HAL open science

Measurement report: Nitrogen isotopes (δ15N) and first quantification of oxygen isotope anomalies (Δ17O, δ18O) in atmospheric nitrogen dioxide

Sarah Albertin, Joël E Savarino, Slimane Bekki, Albane Barbero, Nicolas Caillon

▶ **To cite this version:**

Sarah Albertin, Joël E Savarino, Slimane Bekki, Albane Barbero, Nicolas Caillon. Measurement report: Nitrogen isotopes (δ15N) and first quantification of oxygen isotope anomalies (Δ17O, δ18O) in atmospheric nitrogen dioxide. Atmospheric Chemistry and Physics Discussions, 2021, pp.(Under Review). 10.5194/acp-2020-1143 . insu-03066334v1

HAL Id: insu-03066334

https://insu.hal.science/insu-03066334v1

Submitted on 15 Dec 2020 (v1), last revised 27 Jul 2021 (v3)

HAL is a multi-disciplinary open access archive for the deposit and dissemination of scientific research documents, whether they are published or not. The documents may come from teaching and research institutions in France or abroad, or from public or private research centers.

L'archive ouverte pluridisciplinaire **HAL**, est destinée au dépôt et à la diffusion de documents scientifiques de niveau recherche, publiés ou non, émanant des établissements d'enseignement et de recherche français ou étrangers, des laboratoires publics ou privés.

Distributed under a Creative Commons Attribution - NonCommercial 4.0 International License

https://doi.org/10.5194/acp-2020-1143
Preprint. Discussion started: 14 December 2020
© Author(s) 2020. CC BY 4.0 License.

Atmospheric Chemistry and Physics Discussions

Measurement report : Nitrogen isotopes (δ^{15}N) and first quantification of oxygen isotope anomalies (Δ^{17}O, δ^{18}O) in atmospheric nitrogen dioxide

Sarah Albertin[1,2], Joël Savarino[2], Slimane Bekki[1], Albane Barbero[2] and Nicolas Caillon[2]

[1]LATMOS/IPSL, Sorbonne Université, UVSQ, CNRS, 75005 Paris, France
[2]IGE, Univ. Grenoble Alpes, CNRS, IRD, Grenoble INP, 38000 Grenoble, France

Correspondence to: Sarah Albertin (sarah.albertin@latmos.ipsl.fr)

Abstract. The isotopic composition of nitrogen and oxygen in nitrogen dioxide (NO_2) potentially carries a wealth of information about the dynamics of the nitrogen oxides (NO_x = nitric oxide(NO) + NO_2) chemistry in the atmosphere. While nitrogen isotopes of NO_2 are subtle indicators of emissions, NO_x chemistry and isotopic nitrogen exchange between NO and NO_2, oxygen isotopes are believed to reflect only the O_3/NO_x/VOC chemical regime in different atmospheric environments. In order to access this potential tracer of the tropospheric chemistry, we have developed an efficient active method to trap atmospheric NO_2 on denuder tubes and measured, for the first time, its multi-isotopic composition (δ^{15}N, δ^{18}O, and Δ^{17}O). The δ^{15}N values of NO_2 trapped at our site in Grenoble, France, show little variability (−11.8 to −4.9 ‰) with negligible N isotope fractionations between NO and NO_2 due to high NO_2/NO_x ratios. NO_x emissions main sources are estimated using a stable isotope model indicating the predominance of traffic NO_x emissions in this area. The Δ^{17}O values, however, reveal an important diurnal cycle peaking in late morning at (39.2 ± 1.7) ‰ and decreasing at night until (20.5 ± 1.7) ‰. On top of this diurnal cycle, Δ^{17}O also has substantial variability during the day (from 29.7 to 39.2 ‰), certainly driven by changes in the O_3 to peroxyl radicals ratio. The night-time decay of Δ^{17}O(NO_2) appears to be driven by NO_2 slow removal, mostly from conversion into N_2O_5, and its formation from the reaction between O_3 and emitted NO. Our Δ^{17}O(NO_2) measured towards the end of the night is quantitatively consistent with typical values of Δ^{17}O(O_3). These preliminary results are very promising for using Δ^{17}O of NO_2 as a probe of the atmospheric oxidative activity and for interpreting NO_3^- isotopic composition records.

1 Introduction

Nitrogen oxides (NO_x = NO_2 + NO) are at the heart of tropospheric chemistry, as they are involved in key reaction chains governing the production and destruction of compounds of fundamental interest for health, ecosystems and climate issues (Brown, 2006; Finlayson-Pitts and Pitts, 2000; Jacob, 1999). For example, NO_2 photolysis followed by reaction of NO with peroxy radicals (RO_2 = HO_2 + RO_2) is the only significant source of ozone (O_3) in the troposphere where it serves as a severe air pollutant and a greenhouse gas. Tropospheric O_3 also plays a major role in the production processes of radicals which are responsible for the oxidation and removal of compounds emitted into the atmosphere (Crutzen, 1996). This "cleaning" ability is referred to as the atmospheric oxidative capacity (AOC; Prinn, 2003). Additionally, NO_x species are at the core of the reactive nitrogen cycle as precursors of atmospheric nitrate (particulate NO_3^- + gaseous HNO_3) which contributes to soil

https://doi.org/10.5194/acp-2020-1143
Preprint. Discussion started: 14 December 2020
© Author(s) 2020. CC BY 4.0 License.

acidification and eutrophication (Galloway et al., 2004) and aerosol radiative forcing (Liao and Seinfeld, 2005). In order to better understand the reactive nitrogen (which includes NO_x and HNO_3) chemistry and the related AOC, it is necessary to better constrain individual chemical processes driving NO_x chemistry.

Stable isotopes analysis is a powerful tool for tracing emissions sources, the individual chemical processes and budgets of atmospheric trace gases (Kaye, 1987). Because different processes favour lighter or heavier isotopologues, the isotopic composition of a chemical species will often vary according to the specific physico-chemical and biological processes it has undergone. This phenomenon of isotopic fractionation can thus be used to trace different processes involved in the formation of the chemical species being analyzed. Isotopic enrichment (δ) of an element X is expressed in ‰ and defined as: $\delta^{n}X = ({}^{n}R_{spl}/{}^{n}R_{ref} - 1)$ with ${}^{n}R$ the elemental isotope abundance ratio of the heavy isotope over the light isotope (e.g. for oxygen isotopes ${}^{18}R({}^{18}O/{}^{16}O) \equiv {}^{18}R = x({}^{18}O)/x({}^{16}O)$ or ${}^{17}R({}^{17}O/{}^{16}O) \equiv {}^{17}R = x({}^{17}O)/x({}^{16}O)$, with x the isotopic abundance) in a sample (R_{spl}) and in a reference (R_{ref}). The Vienna Standard Mean Ocean Water (VSMOW; Li et al., 1988) and atmospheric nitrogen (N_2; Mariotti, 1984) are the international references for oxygen and nitrogen ratios, respectively. Most natural isotopic fractionations are mass dependent fractionations (MDF; Urey, 1947), as it is notably the case for terrestrial oxygenated species in which the triple oxygen composition follows $\delta^{17}O \approx 0.52 \times \delta^{18}O$ (Thiemens, 1999). Yet, laboratory experiments (Thiemens and Heidenreich, 1983) and atmospheric observations (Johnston and Thiemens, 1997; Krankowsky et al., 1995; Vicars and Savarino, 2014) have showed that the isotopic composition of ozone formed in the atmosphere does not follow this canonical MDF relationship and reflects mass independent fractionation (MIF) processes. The important deviation from the MDF oxygen relationship is called the oxygen-17 anomaly ($\Delta^{17}O$) and is defined here in its approximate linearized form as $\Delta^{17}O = \delta^{17}O - 0.52 \times \delta^{18}O$. Our choice of this linear definition is mainly motivated by its convenience for mass balance calculations and its validity for our large $\Delta^{17}O$ values and variability. Overall, biases related to our choice of the linear definition are marginal in our conditions (Assonov and Brenninkmeijer, 2005). It follows that $\Delta^{17}O$ inherited from ozone can be considered as conserved during MDF processes.

The multi-isotopic composition of NO_x is therefore a very valuable tracer of its emissions and chemistry in the atmosphere. However, so far, $\Delta^{17}O$ of atmospheric NO_2 ($\Delta^{17}O(NO_2)$) has been investigated only using laboratory (Michalski et al., 2014) and modelling (Alexander et al., 2009, 2020; Lyons, 2001; Morin et al., 2011) approaches with theoretical frameworks, and these results need to be tested against atmospheric observations. Walters et al. (2018) have presented a method of sampling and analysing nitrogen ang oxygen stable isotopes of NO_2 collected separately at daytime and nighttime in an urban area but they did not report on $\Delta^{17}O$. Dahal and Hastings (2016) have attempted to measure $\Delta^{17}O$ of NO_2 collected on passive samplers, but the isotopic signal was partly degraded during the sampling and the analytical procedures. Building on their work, we present here an efficient method to collect atmospheric NO_2 for isotopic analysis and present the first measurements of triple oxygen isotopes and double nitrogen isotopes of atmospheric NO_2. After estimating the nitrogen isotopic fractionation between NO and NO_2, we infer from $\delta^{15}N$ of the NO_2 ($\delta^{15}N(NO_2)$) the major emissions sources of NO_x influencing our sampling site using a stable isotope model (EPA IsoSource Model, 2003). Combined with mass-balance equations, oxygen isotopes are used

https://doi.org/10.5194/acp-2020-1143
Preprint. Discussion started: 14 December 2020
© Author(s) 2020. CC BY 4.0 License.

to investigate the links between the variability of the oxygen isotope anomaly of NO_2 and its formation pathways. We also revisit the Morin et al. (2011) NO_x isotopic theoretical framework and extend it to urban environments.

2 Materials and Methods

2.1 Sampling method

NO_2 was sampled on an active (pumped) collection system using denuder tubes. This method is more efficient to collect NO_2 than passive methods (Røyset, 1998), allowing for shorter collection times with a breakthrough of the absorption capacity below 1 %. (Buttini et al., 1987; Williams and Grosjean, 1990). The sampled air was pumped through a ChemComb™ 3500 speciation cartridge (Thermo Scientific™, USA). Initially used for the speciation of gases and aerosols, these advanced sampling platforms consist of a $PM_{2.5}$ impactor inlet connected to a stainless-steel cylinder that contains two glass honeycomb denuders connected in series for gas collection and a Teflon stage filter pack for aerosols. To collect NO_2, glass tubes were coated with an alkaline guaiacol solution. In basic medium, guaiacol (IUPAC name: 2-Methoxyphenol) is known to react with NO_2 to form stable NO_2^- ions (Nash, 1970) that preserve the original NO_2 isotopic signal due to the basic nature of the medium (pH = 14 after 10 ml extraction). Because NO or peroxyacetyl nitrate (PAN) are not collected by guaiacol, this methodology avoids potential interference from these compounds in later analyses (Buttini et al., 1987). Although nitrous acid (HONO) can bind as NO_2^-, it is unlikely to adversely impact the results as its concentration is much lower than NO_2 (by a factor of 10 to 20) even in very polluted cities (Harris et al., 1982).

To evaluate the sampling system performance, a series of experiments were run with artificial gaseous NO_2. Using a commercial gas standard generator (KinTek FlexStream™) feed with zero-air, artificial NO_2 (Metronics Dynacal™) was sent through a ChemComb cartridge while NO_x concentration was measured up- and down-stream of the cartridge. From 1 to 30 nmol mol^{-1} of NO_2 (representative of rural to urban atmospheric conditions), concentrations coming out of the cartridge were never above the noise level of the NO_x monitor (2.5 nmol mol^{-1}). To estimate the denuders trapping efficiency, we passed different concentrations of gaseous NO_2 through the collection apparatus and measured the amount of NO_2^- collected on the two denuders both connected in series. The denuder efficiency E was then calculated according to the following equation (Buttini et al., 1987):

$$E = (1 - \frac{b}{a}) \times 100\ \% \qquad (1)$$

with a and b representing the amount of NO_2^- collected on the first and the second denuder, respectively. From 0.3 to 1.3 µmol of NO_2 generated (see Fig. 1), the mean E value was about (97 ± 3) %. The amount of NO_2^- measured on second denuders were reproducible and equivalent to blanks, representing on average 3 % of the quantity measured on the first denuders. In light of these results, denuders in second position were not subjected to isotopic analysis and allowed trapping efficiency control.

https://doi.org/10.5194/acp-2020-1143
Preprint. Discussion started: 14 December 2020
© Author(s) 2020. CC BY 4.0 License.

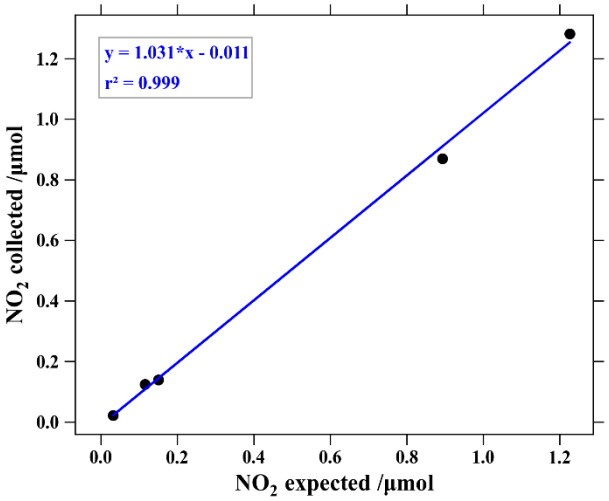

Figure 1: Correlation plot of NO_2 collected on the first denuder tube of the sampling cartridge vs. NO_2 produced by the gas standard generator.

2.2 Isotopic analysis

Simultaneous isotopic analyses of $\delta^{15}N$, $\delta^{18}O$, and $\delta^{17}O$ were performed using a Finnigan™-MAT253 isotope ratio mass spectrometer (IRMS) following techniques described by Casciotti et al. (2002) and Kaiser et al. (2007). The azide method (McIlvin and Altabet, 2005) was used where ≈ 100 nmol of nitrites was converted to N_2O using a 50:50 by volume mixture of 2M sodium azide and 100 % acetic acid. The principle of identical treatment (Brand, 1996) was strictly respected where the standards and samples possessed the same nitrite concentration, water isotopes, total volume and matrix. Three international KNO_2 salts standards, RSIL-N7373, RSIL-N10219, and RSIL-N23 with respective $\delta^{15}N/\delta^{18}O$ values of –79.6/4.2 ‰, 2.8/88.5 ‰, and 3.7/11.4 ‰ were used for normalisation of δ-scale. Scale contraction factors were obtained with the linear regression between measured and known values of $\delta^{15}N$ and $\delta^{18}O$. Although the three standards cover a wide range of isotopic composition in $\delta^{15}N$ and $\delta^{18}O$, they do not have an isotopic anomaly in ^{17}O. For $\delta^{17}O$-scale, MDF fractionation slope (0.52) is assumed for two of these laboratory-prepared nitrite standards (see Appendix A for more details). Accuracy of this analytical method on $\delta^{17}O$, $\delta^{18}O$ and $\delta^{15}N$ measurements was estimated as the standard deviation (σ) of the residuals between our measurements of the RSIL standards and their expected values. Additionally, isotopic integrity from denuders extraction to the analysis by IRMS has been investigated and showed no degradation over several weeks (see Appendix B) confirming that this method is suitable for isotopic analysis of NO_2, as first demonstrated by Walters et al. (2018). The uncertainties applied to our measurements of $\delta^{15}N$, $\delta^{17}O$ and $\delta^{18}O$ are reported as the propagation error of the measurement uncertainty and the uncertainty resulting from sample storage. Uncertainty on $\Delta^{17}O$ is derived from the propagation error of the overall uncertainty on $\delta^{17}O$ and $\delta^{18}O$. In our study, average uncertainties on $\delta^{15}N$, $\delta^{17}O$, $\delta^{18}O$, and $\Delta^{17}O$ are estimated to be ± 0.1, ± 1.1, ± 2.5 and ± 1.7 ‰, respectively (1σ uncertainties).

https://doi.org/10.5194/acp-2020-1143
Preprint. Discussion started: 14 December 2020
© Author(s) 2020. CC BY 4.0 License.

2.3 Study site and atmospheric NO_2 collection

Atmospheric NO_2 was collected at the Université Grenoble Alpes campus site. Located to the eastern Grenoble urban area (690 000 inhabitants), the campus stands between a major transportation route and the Isère river. The city is located at the confluence of three valleys surrounded by mountain chains that influence the atmospheric dynamics and the local air quality. During winter, persistent temperature inversions combined with intense domestic heating can lead to severe PM_{10} pollution events (Largeron and Staquet, 2016) with daily-average concentration above World Health Organisation thresholds. In summer, emissions are mainly controlled by road traffic that can result in heightened ozone concentrations, especially during stagnant conditions.

Sampling was conducted on a platform five meters above the ground surface. Ambient air was drawn through the cartridge with a Millipore vacuum pump at a flow rate of 10 L min^{-1} (room temperature and one atmospheric pressure) adjusted using a Cole-Parmer™ flowmeter (accuracy ± 3 %). Samples were collected during 24 hours with 3 h sampling intervals during the day and 5 h sampling from midnight to 5:00 am in order to capture the daily variability in NO_2 isotopic composition. Ambient NO and NO_2 concentrations were measured with a 2B Technologies™ NO monitor model 410 paired with a NO_2 converter model 401.

Honeycomb denuders were cleaned and coated the day before sampling. After being generously rinsed (5 minutes under a stream of deionised water), the denuders were placed in a vacuum chamber (Thermo Scientific™ Refrigerated VaporTrap paired with a SpeedVac Concentrator) and dried at 40 °C during 1 hour. Then, denuders internal walls were individually coated with 10 ml of a 95:5 by volume mixture of 2.5 M KOH (prepared in methanol) and ultrapure guaiacol prepared daily. Denuders were then drawn off, dried in the vacuum chamber at 40 °C during 30 minutes to minimize blanks, hermetically sealed and stored at ambient temperature in the dark until usage. The different components of the cartridge (impactor, filters, denuders) were cleaned, dried and fitted together just before use. At the end of the sampling period both denuders were removed from the ChemComb cartridge and rinsed with 10 ml of deionised water in order to leach trapped NO_2 out. 1 ml of the eluent was rapidly used to determine the nitrite concentration using the Griess-Saltzman reaction and UV-vis spectrometry at 520 nm. Recovered eluent (≈ 7 ml by denuder) was poured in a labelled 15 ml corning® and stored in a freezer until isotopic analysis the following days.

3 Atmospheric observations and multi-isotopic measurements

3.1 NO_x and O_3 atmospheric observations

Figure 2 shows the time evolution of the hourly NO_2, NO and O_3 mixing ratio measured during the period covering two nights and one day (from 15 May 2019 21:00 to 16 May 2019 5:00). Note that most of our NO measurements are found to be within the reported detection limit of the instrument except in the morning (see Table 1) and therefore have to be treated with lot of caution. NO_2 mixing ratios during the sampling period ((5.7 ± 4.3) nmol mol^{-1}; mean ± one standard deviation) are in good

https://doi.org/10.5194/acp-2020-1143
Preprint. Discussion started: 14 December 2020
© Author(s) 2020. CC BY 4.0 License.

agreement with the range of values measured at the local air quality site located a kilometre south of the sampling site (https://www.atmo-auvergnerhonealpes.fr/).

During both nights, most of the NO_x are in the form of NO_2. After sunrise, there is rapid interconversion between NO and NO_2, driven by NO_2 photolysis and reactions of NO with O_3 and peroxy radicals (Jacob, 1999). NO_2 levels are maximum on 15 May between 4:00 and 10:00 with a sharp peak of 19 nmol mol^{-1} at 8:00. After the morning rise, NO_2 decreases to reach a background concentration of about (2.7 ± 0.2) nmol mol^{-1}. This diurnal variation is common in urban/suburban sites characterised by a morning peak caused by important NO_x emissions, mainly from road traffic (Mayer, 1999). As morning progresses, the boundary layer height increases rapidly, favouring fast dilution of NO_x concentrations. Moreover, during the day, NO_2 is converted to HNO_3, notably by its reaction with OH radicals. Thus, NO_x concentration remains low during the day likely because of the combination of atmospheric dilution by vertical mixing and efficient chemical conversion by OH and organic radicals (Tie et al., 2007). In dense urban areas, a second NO_x traffic emission peak can occur in late afternoon but it is not observed at our sampling site for that specific day. This surface pollution peak is usually weaker than the morning peak due to an elevated boundary layer and a wider period of evening commute. After sunset, NO_2 concentrations increase gently and reach a smooth peak with a maximum of 11 nmol mol^{-1} around 1:00 am local time, also recorded at the local air quality site. This NO_2 concentration rise may be due to low NO emissions (converted to NO_2 by reaction with O_3) combined with a decreasing boundary layer height during the night which traps atmospheric species close to the surface (Tie et al., 2007; Villena et al., 2011).

Ozone also exhibits a diurnal variation typical of urban areas (Velasco et al., 2008). O_3 peaks around 50 nmol mol^{-1} at the beginning of both nights to then declines continuously. Indeed, after sunset, O_3 production ceases and its concentration drops due to its dry deposition, reactions with organics, and O_3 titration by NO emitted from evening traffic, heating, and industrial activities in the stable nocturnal boundary layer (Klein et al., 2019). O_3 reaches a minimum (about 15 nmol mol^{-1}) not at the end of the night but during the morning rush hours peak of NO. O_x (= O_3 + NO_2) is a more conservative quantity than O_3 because it is less affected by conversion of O_3 into NO_2 through NO titration which is important in urban environments (Kleinman et al., 2002). For instance, between 6:00 and 8:00 am, O_3 is strongly titrated by freshly emitted NO with its concentration dropping to about 15 nmol mol^{-1} while O_x reaches a moderate minimum of 34 nmol mol^{-1}. After this morning drop, O_3 recovers rapidly to about 35 nmol mol^{-1} in the late morning, possibly caused by downward O_3 flux associated with the formation of the day-time thick boundary layer (Jin and Demerjian, 1993; Klein et al., 2019). During the rest of the day, O_3 and O_x keep increasing gently due to photochemical production and reach a close maxima at the end of the afternoon (Geng et al., 2008). After sunset, the important decline of both O_3 and O_x highlights the physical losses, notably O_3 deposition, and chemical loss of NO_x, typical of urban area.

https://doi.org/10.5194/acp-2020-1143
Preprint. Discussion started: 14 December 2020
© Author(s) 2020. CC BY 4.0 License.

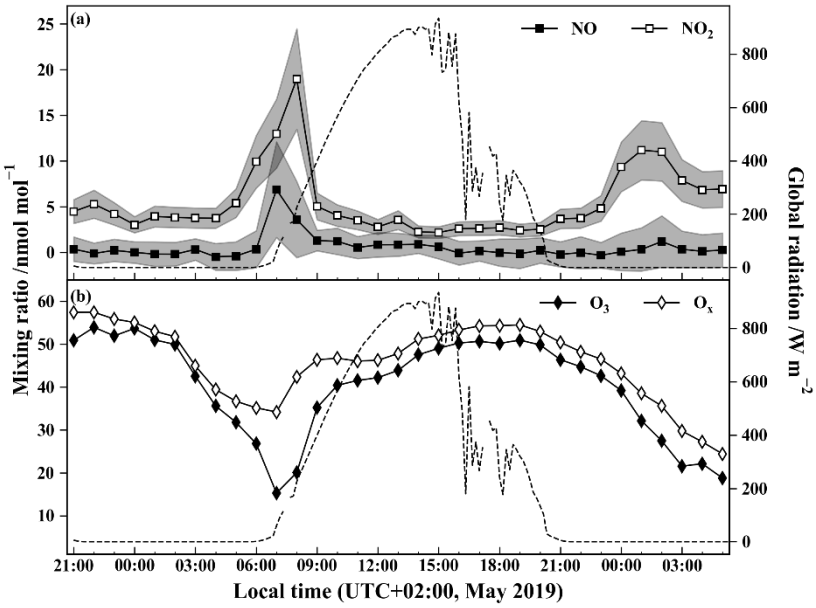

Figure 2: Temporal evolution of (a) NO (closed squares) and NO_2 (open squares) at the sampling site (the grey envelops represent ± 1σ variations over 1 hour) and of (b) O_3 (close diamonds) and O_x (= O_3 + NO_2; open diamonds) at the air quality station during sampling. Markers represent for (a) the hourly mean derived from 1-min measurements and for (b) hourly mean provided by the air quality station. Global solar radiation measured at 200 meters from the sampling site is represented by dashed lines.

3.2 Multi-isotopic composition measurements of atmospheric NO_2

We present the data for the multi-isotopic composition of seven atmospheric NO_2 samples while two additional samples were rejected as NO_2^- amounts were too low to perform a reliable analysis. Table 1 reports ambient mean concentrations of NO, NO_2 and O_3 for the isotopic sampling intervals and corresponding measured NO_2 isotopic composition ($\delta^{15}N_{mes}$, $\delta^{18}O_{mes}$, and $\Delta^{17}O_{mes}$). Figure 3 depicts the time series of measured $\delta^{15}N$, $\delta^{18}O$, and $\Delta^{17}O$ of atmospheric NO_2. The temporal evolution of NO_2 nitrogen and oxygen isotopic composition is interpreted in the following section.

https://doi.org/10.5194/acp-2020-1143
Preprint. Discussion started: 14 December 2020
© Author(s) 2020. CC BY 4.0 License.

Sampling date & time (start - end)	NO (± 2.5 nmol mol^{-1})	NO_2 (± 2.5 nmol mol^{-1})	O_3 (*) (± 6.8 nmol mol^{-1})	$\delta^{15}N_{mes}$ (± 0.1 ‰)	$\delta^{18}O_{mes}$ (± 2.5 ‰)	$\Delta^{17}O_{mes}$ (± 1.7 ‰)
14/5/19 21:00 - 00:00	0.2	4.7	52.3	–11.7	75.6	27.4
15/5/19 06:00 - 09:00	3.6	14.0	20.7	–4.9	97.6	31.8
15/5/19 09:00 - 12:00	1.0	4.2	39.1	–10.1	114.5	39.2
15/5/19 12:00 - 15:00	0.9	2.9	44.6	–11.8	90.9	35.8
15/5/19 15:00 - 18:00	0.3	2.5	50.0	–11.0	86.9	31.1
15/5/19 18:00 - 21:00	0.0	2.6	50.3	–11.1	77.1	29.7
16/5/19 00:00 - 05:00	0.3	8.9	26.9	–11.1	62.2	20.5

Table 1: Summary table of sampling periods (dates, local times), NO, NO_2 and O_3 mean mixing ratios over the collection periods, and calibrated isotopic measurements of $\delta^{15}N$, $\delta^{18}O$, and $\Delta^{17}O$. All the sampling periods lasted 3 hours except the last one that lasted 5 hours. Averaged measurement uncertainties are provide just below the species names. (*) Data monitored at the local air quality site of Saint-Martin d'Hères located a kilometre south of the sampling site (https://www.atmo-auvergnerhonealpes.fr/)

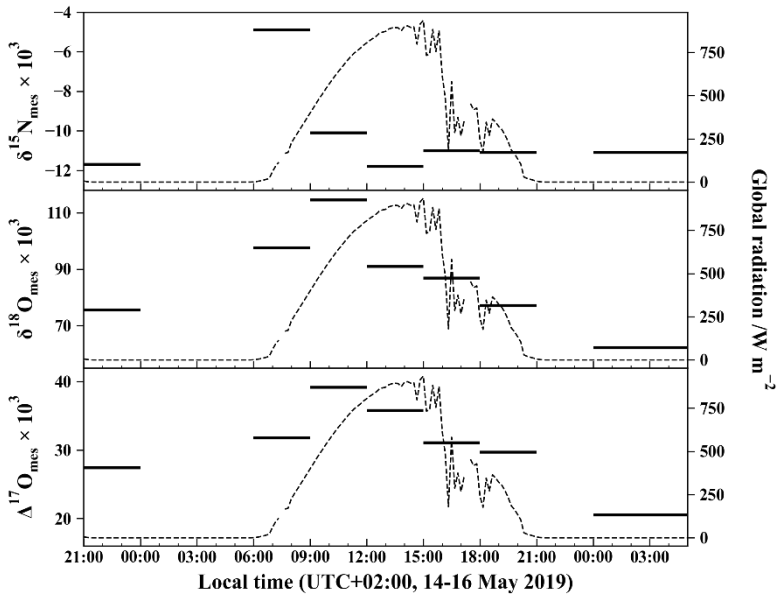

Figure 3: Temporal evolution of $\delta^{15}N$, $\delta^{18}O$ and $\Delta^{17}O$ of atmospheric NO_2 measured with the azide method. Isotopic values for each 3 hours slots are from the same NO_2 sample collected over the 3 hours sampling period (except for the last period which lasts 5 hours). Global solar radiation measured close to the sampling site is represented by dashed lines.

https://doi.org/10.5194/acp-2020-1143
Preprint. Discussion started: 14 December 2020
© Author(s) 2020. CC BY 4.0 License.

4 Discussion of the multi-isotopic composition of atmospheric NO_2

4.1 Nitrogen isotope composition

Measured $\delta^{15}N(NO_2)$ values range from –4.9 to +11.8 ‰ with no clear diurnal variation and values clustering around an overall mean of (–10.2 ± 2.2) ‰ (see Fig. 3). Using a similar method, Walters et al. (2018) collected atmospheric NO_2 over one month in a urban/sub-urban location during the summer. They reported a mean $\delta^{15}N$ value of (–11.4 ± 6.9) ‰, very close to our mean value but with a wider overall range (from –31.4 to +0.4 ‰). In another urban area but using passive samplers, Dahal and Hastings (2016) reported mean $\delta^{15}N(NO_2)$ values of (–8.3 ± 0.9) ‰ and (–6.4 ± 1.4) ‰ for summer and winter periods, respectively. All these values are within the $\delta^{15}N$ range for NO emitted by industrial combustion and traffic sources which are reported to vary from –19.7 to –13.7 ‰ and from –9 to –2 ‰ respectively (Miller et al., 2017; Walters et al., 2015). Interestingly, all the $\delta^{15}N$ values measured at our sampling site fall within a narrow range, from about –12 to –10 ‰, except for the sample collected between 6:00 and 9:00 which has a much higher value of –4.9 ‰. This singular value is well correlated with the morning NO traffic emission spike (see Fig. 2). However, once emitted into the atmosphere, NO can undergo isotopic fractionations that modify the nitrogen isotope distribution in NO_2 relative to emitted NO (Freyer et al., 1993). In order to use $\delta^{15}N(NO_2)$ as a tracer of NO_x sources, we need to quantify these nitrogen isotopic shifts to correct measured $\delta^{15}N(NO_2)$. Nitrogen isotopic fractionation is the result of a combination of two effects: 1) an Equilibrium Isotopic Effect (EIE) between NO and NO_2 and 2) a Leighton Cycle Isotopic Effect (LCIE) due to nitrogen isotopic fractionations during NO oxidation by O_3 and RO_2, and NO_2 photolysis. Recent laboratory experiments reported EIE and LCIE fractionation factors of 1.0289 ± 0.0019 and 0.990 ± 0.005 (Li et al., 2020). Using these fractionation factors, the nitrogen isotopic shift of NO_2 relative to emitted NO_x, defined as $\Delta(NO_2 - NO_x) = \delta^{15}N(NO_2) - \delta^{15}N(NO_x)$, can be estimated at steady state from the following relationship (derived using equation (8) in Li et al., 2020 and assuming $1 + \delta^{15}N(NO_2) = 1$):

$$\Delta(NO_2 - NO_x) = \frac{\alpha_{LCIE} \times A + (\alpha_{EIE} - 1)}{A + 1} \times (1 - f_{NO_2}) \quad (2)$$

$$\text{with } A = \frac{k_{NO+O_3}[O_3]}{k_{NO+NO_2}[NO_2]} \quad (3)$$

where $f_{NO2} = [NO_2]/[NO_x]$, and α_{LCIE} and α_{EIE} are LCIE and EIE fractionation factors. A is defined as the relative contribution of NO_2 isotopic exchanges via LCIE and EIE in the NO_2 lifetime. Note that Eq.(3) does not consider the conversion of NO to NO_2 by RO_2 which could lead to uncertainty on the NO_2 shift when this pathway becomes important with respect to the NO conversion by O_3. Nonetheless, Li et al. (2020) pointed out close agreement between values calculated using Eq.(2) and field isotopic measurements, suggesting that the NO + RO_2 (including HO_2) reactions might have a fractionation factor similar to the one of NO + O_3 reaction. Figure 4 presents the time evolution of hourly $\Delta(NO_2 - NO_x)$ calculated from Eq.(2) and f_{NO2}. Overall, nitrogen oxide isotope effects appear to induce very small $\Delta(NO_2 - NO_x)$ (see Fig. 4). They are found to be negligible during the entire sampling period, except between 7:00 and 9:00 when hourly $\Delta(NO_2 - NO_x)$ ranges from 0.5 to 2.3 ‰. This

https://doi.org/10.5194/acp-2020-1143
Preprint. Discussion started: 14 December 2020
© Author(s) 2020. CC BY 4.0 License.

largely reflects the fact that NO_x is mostly under the form of NO_2 (f_{NO2} = 1) except in the morning (see Fig. 2) due to direct emissions of NO which decreases f_{NO2} (0.87 < f_{NO2} < 0.97 between 7:00 and 9:00; see Fig. 2). Our values are in good agreement with the $\Delta(NO_2 - NO_x)$ range (between 1.3 and 2.5 ‰) calculated from isotopic measurements at West Lafayette, USA (Walters et al., 2018). Moreover, Li et al. (2020) calculated a mean $\Delta(NO_2 - NO_x)$ of (1.3 ± 3.2) ‰ from isotopic measurements near San Diego, USA (NO_x concentration varied from 1 to 9 nmol mol^{-1}). Overall, it appears that, in moderately polluted environments, the small $\Delta(NO_2 - NO_x)$ values are mostly due to high f_{NO2}. In our case, the isotopic correction factor is only significant for the sample collected between 6:00 and 9:00 to which we apply a 3 h mean correction factor of 1.0 ‰. This lowers $\delta^{15}N(NO_2)$ from –4.9 to –5.9 ‰ but it still remains distinctively higher than for the other sampling time intervals.

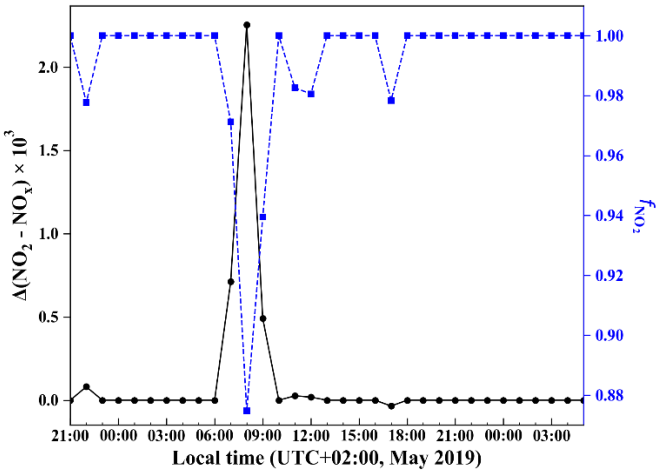

Figure 4: Calculated isotopic fractionation values between NO_2 and NO_x ($\Delta(NO_2 - NO_x)$, solid black line) using Eq.(2) and f_{NO2} (dashed blue line) during our sampling period.

Having accounting for isotope fractionation effects, we can assess the main possible NO_x sources contribution at our site using the US EPA source partitioning model IsoSource (EPA IsoSource Model, 2003) which solves numerically the following two-equation system:

$$\delta^{15}N(NO_2) = \sum_i (f_i \times \delta^{15}N_i(NO_x)) \quad (4)$$

$$\sum_i f_i = 1 \quad (5)$$

with f_i the contribution proportion of source i and $\delta^{15}N_i(NO_x)$ the nitrogen isotopic composition of the NO_x source i. We input the isotopic signature of each sources influencing the nitrogen isotopic composition of NO_2 and here we differentiate biogenic, fuel combustion and traffic sources of NO_x with distinctive $\delta^{15}N$ means of –53.6, –17.9 and –2 ‰ respectively (Walters et al., 2018). We set the source increment to 1 % and the mass balance tolerance of ± 5 %. As output, the model provides the most feasible source combinations and the descriptive statistics on the distribution for each source (Phillips and Gregg, 2003). According to the model results (see Fig. 5), traffic NO_x emissions are dominant with a mean relative contribution of 0.82 ±

https://doi.org/10.5194/acp-2020-1143
Preprint. Discussion started: 14 December 2020
© Author(s) 2020. CC BY 4.0 License.

0.05 during the morning early hours against 0.62 ± 0.12 for the rest of the sampling period. Outside of traffic, fuel combustion and biogenic sources account respectively for only 0.16 ± 0.08 and 0.03 ± 0.02 in the early morning against 0.29 ± 0.17 and 0.09 ± 0.05 for the rest of the sampling period. A very recent study (Barré et al., 2020) has estimated NO_2 changes during the COVID-19 lockdown combining satellite data (from the Tropospheric Monitoring Instrument), surface measurements and simulations (from the Copernicus Atmospheric Monitoring Service) and considering for weather variability that could bias the estimates. Interestingly, this study shows a NO_2 reduction estimates around 50 % in Lyon, France during the lockdown period in comparison of pre-lockdown concentration. If not strictly extrapolable to Grenoble because Lyon has a larger urban area (2 300 000 inhabitants), the NO_2 column change in Lyon and the relative contribution of traffic in Grenoble NO_x sources (68 %) inferred from N isotope values of NO_2 are surprisingly close and comfort the idea that $\delta^{15}N$ of NO_2 is a very reliable tracer of NO_x emission sources after correction for LCIE and EIE.

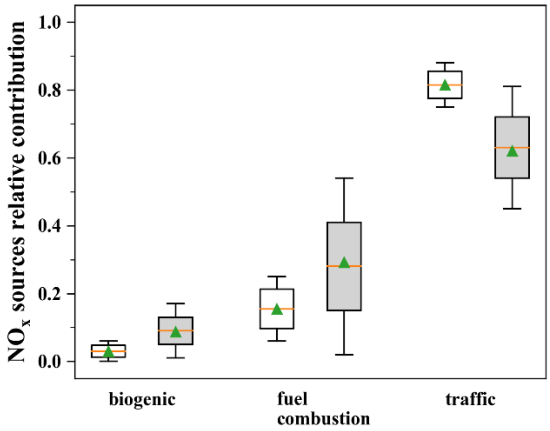

Figure 5: NO_x emission source partitioning using the IsoSource EPA Model based on $\delta^{15}N(NO_2)$ measured during: the morning rush hours from 6:00 to 9:00 am local time (white boxes) and the other 3 h intervals (grey boxes). References values for each sources were taken from Walters et al. (2018).

4.2 Oxygen isotope composition

The time evolution of $\delta^{18}O$ of atmospheric NO_2 ($\delta^{18}O(NO_2)$) shown in Fig. 3 exhibits a substantial diurnal variation with a day mean of (93.4 ± 13.9) ‰ and night mean of (68.9 ± 9.5) ‰. A maximum value of 114.5 ‰ is observed in the morning (09:00-12:00 interval) and a minimum value of 62.2 ‰ for the late-night interval (00:00-05:00). Using a similar sampling apparatus during summer in the urban/sub-urban site of West Lafayette, USA, Walters et al. (2018) reported $\delta^{18}O(NO_2)$ daytime and nighttime mean values of (86.5 ± 14.1) ‰ and (56.3 ± 7.1) ‰, respectively. Although our daytime values are higher than those of Walters et al. (2018), both datasets exhibit the same day-night contrast with a maximum during the day and a minimum at night. As expected from $\delta^{18}O$ values, $\Delta^{17}O(NO_2)$ follows a similar diurnal variation with a maximum value of 39.2 ‰ for

https://doi.org/10.5194/acp-2020-1143
Preprint. Discussion started: 14 December 2020
© Author(s) 2020. CC BY 4.0 License.

the 09:00-12:00 interval and a minimum value of 20.5 ‰ for the 00:00-05:00 interval. High $\Delta^{17}O$ values are expected to reflect the importance of ozone in the oxidation of NO to NO_2. Since daytime and nighttime chemistries are radically different, interpretation of our $\Delta^{17}O$ measurements and their implications are discussed separately by day and night.

4.2.1 Fundamentals of NO_x chemistry and isotopic transfers

NO_x are mainly produced under the form of NO by combustion and lighting processes (Dennison et al., 2006; Young, 2002) and by the biological activity of soils (Davidson and Kingerlee, 1997). In the daytime, NO and NO_2 rapidly interconvert in a time scale of about 1-2 minutes establishing a photostationary steady state (PSS; Leighton 1961):

$$NO_2 + h\nu \xrightarrow{M} O(^3P) + NO \quad \text{(R1)}$$

$$O(^3P) + O_2 \xrightarrow{M} O_3 \text{ with } M = N_2 \text{ or } O_2 \quad \text{(R2)}$$

$$NO + O_3 \rightarrow NO_2 + O_2 \quad \text{(R3)}$$

This so-called null cycle can be disturbed by RO_2 radicals when NO_x concentration are relatively high, typically above 30 pmol mol^{-1} (Seinfeld and Pandis, 2006):

$$NO + RO_2 \rightarrow NO_2 + RO \quad \text{(R4)}$$

The reaction between NO and RO_2 competes with the NO + O_3 reaction, allowing NO_2 formation without the consumption of an ozone molecule in the cycle (Monks, 2005). This results in ozone production and can lead to severe ozone build up in polluted areas. At night, RO_2 concentrations are strongly reduced making ozone the main NO oxidant following R3. NO_x are mainly removed from the atmosphere via the oxidation of NO_2 into nitric acid during the day:

$$NO_2 + OH \rightarrow HNO_3 \quad \text{(R5)}$$

and at night :

$$NO_2 + O_3 \xrightarrow{M} NO_3 + O_2 \quad \text{(R6)}$$

$$NO_3 + NO_2 \xrightarrow{M} N_2O_5 \xrightarrow{H_2O,\ aerosol} 2\ NHO_3 \quad \text{(R7)}$$

In this framework, $\Delta^{17}O(NO_2)$ is driven by the relative importance of the different NO_2 production channels because NO_2 loss processes do not fractionate in terms of oxygen mass-independent anomaly. Each NO_2 production channel generates a specific mass-independent isotopic anomaly $\Delta^{17}O$ on the produced NO_2 (Kaiser et al., 2004). Based on the NO_2 continuity equation, this can be expressed with the following $\Delta^{17}O(NO_2)$ mass-balance equation (Morin et al., 2011):

$$\frac{d}{dt}\left([NO_2] \times \Delta^{17}O(NO_2)\right) = \sum_i \left(P_i \times \Delta^{17}O_i(NO_2)\right) - \left(\sum_j L_j\right) \times \Delta^{17}O(NO_2) \quad (6)$$

https://doi.org/10.5194/acp-2020-1143
Preprint. Discussion started: 14 December 2020
© Author(s) 2020. CC BY 4.0 License.

with [NO_2] being the atmospheric NO_2 concentration, P_i and L_j the NO_2 production/emission and loss rates (= concentration of involved species multiplied by the kinetic constants of the considered chemical reaction), and $\Delta^{17}O_i(NO_2)$ the specific isotope anomaly transferred to NO_2 through the production reaction *i*.

4.2.2 $\Delta^{17}O_{day}(NO_2)$

By day, the NO_x photochemical cycle (R1 to R4) achieves a steady state in 1-2 minutes, which is several orders of magnitude faster than NO_2 loss reactions (Atkinson et al., 1997) and emission rate (NO_x are mainly emitted under the form of NO; Villena et al., 2011). It follows that NO and NO_2 short variations can be neglected i.e. $\frac{d}{dt}[NO_2] \approx 0$ and $\frac{d}{dt}[NO] \approx 0$ on short timescales. In addition, fast interconversions between NO and NO_2 generate quickly an isotopic equilibrium between NO and NO_2 resulting in $\Delta^{17}O(NO_2) \approx \Delta^{17}O(NO)$ (Michalski et al., 2014; Morin et al., 2007). With these approximations, considering only the main reactions and neglecting halogen chemistry, Eq.(6) yields to (Morin et al., 2007):

$$\Delta^{17}O_{day}(NO_2) \approx \frac{k_{NO+O_3}[O_3] \times \Delta^{17}O_{NO+O_3}(NO_2) + k_{NO+RO_2}[RO_2] \times \Delta^{17}O_{NO+RO_2}(NO_2)}{k_{NO+O_3}[O_3] + k_{NO+RO_2}[RO_2]} \quad (7)$$

with $\Delta^{17}O_{NO+O3}(NO_2)$ being the ozone isotopic anomaly transferred to NO during its oxidation to NO_2 via R3 (also called the transfer function of the isotope anomaly of ozone to NO_2; Savarino et al., 2008) and $\Delta^{17}O_{NO+RO2}(NO_2)$ being the RO_2 isotopic anomaly transferred to NO during its oxidation to NO_2 via R4. $\Delta^{17}O_{NO+RO2}(NO_2)$ can be considered to be negligible (Alexander et al., 2020; Michalski et al., 2003) because RO_2 are mainly formed by the reactions R + O_2 and H + O_2 and the isotopic anomaly of atmospheric O_2 is very close to 0 ‰ (Barkan and Luz, 2003). This assumption has been estimated to affect the overall $\Delta^{17}O$ of RO_2 values by less than 1 ‰ (Röckmann et al., 2001). As a result, Eq.(7) can be simplified, giving a $\Delta^{17}O_{day}(NO_2)$ driven by the relative importance of R3 (NO + O_3) and R4 (NO + RO_2) in the NO oxidation and by the oxygen isotopic anomaly transferred from O_3 to NO_2:

$$\Delta^{17}O_{day}(NO_2) \approx \alpha \times \Delta^{17}O_{NO+O_3}(NO_2) \quad (8)$$

$$\text{with } \alpha = \frac{k_{NO+O_3}[O_3]}{k_{NO+O_3}[O_3] + k_{NO+RO_2}[RO_2]} \quad (9)$$

$\Delta^{17}O_{NO+O3}(NO_2)$ has been determined experimentally by Savarino et al. (2008). They reported $\Delta^{17}O_{NO+O3}(NO_2) = (1.18 \pm 0.07 \times \Delta^{17}O(O_3) + 6.6 \pm 1.5)$ with $\Delta^{17}O(O_3)$ being the bulk ozone isotopic anomaly. $\Delta^{17}O(O_3)$ has been measured in Grenoble in 2012 (Vicars and Savarino, 2014); the mean measured $\Delta^{17}O(O_3)$ was (26.2 ± 1.3) ‰ corresponding to a $\Delta^{17}O_{NO+O3}(NO_2)$ value of (37.5 ± 2.8) ‰ which, according to Eq.(8), would give a maximum $\Delta^{17}O_{day}(NO_2)$ value of (37.5 ± 2.8) ‰. It is consistent with our maximum measured $\Delta^{17}O(NO_2)$ value of 39.2 ‰ for the 09:00-12:00 interval. In light of the known uncertainties, the small difference is not significant and is much smaller than the diurnal variations of $\Delta^{17}O(NO_2)$. Note that the $\Delta^{17}O$ calibration is not very accurate for the most enriched samples because nitrite standards with high $\Delta^{17}O$ are still not readily available. In a laboratory study Michalski et al. (2014) measured the $\Delta^{17}O$ of NO_2 formed by the photochemical NO-NO_2-O_3 cycle and

https://doi.org/10.5194/acp-2020-1143
Preprint. Discussion started: 14 December 2020
© Author(s) 2020. CC BY 4.0 License.

reported $\Delta^{17}O(NO_2)$ = (39.3 ± 1.9) ‰. Despite experimental conditions (e.g. $NO_x \gg O_3$, light source, absence of VOCs) that are not strictly applicable to our atmospheric conditions, their value is surprisingly close to our maximum value. Assuming that our maximum $\Delta^{17}O(NO_2)$ value correspond to α close to unity (R3 ($NO + O_3$) ≫ R4 ($NO + RO_2$)), we use a value of 39.2 ‰ for $\Delta^{17}O_{NO+O3}(NO_2)$ for the following calculations. Combining Eq.(8) and Eq.(9), an expression for the RO_2 concentration can be derived as:

$$[RO_2] = \frac{k_{NO+O_3} \times [O_3]}{k_{NO+RO_2}} \left(\frac{\Delta^{17}O_{NO+O_3}(NO_2)}{\Delta^{17}O_{day}(NO_2)} - 1\right) \quad (10)$$

Figure 6 shows the estimated daytime evolution of α and RO_2. α varies between 0.76 and 1 with a mean daytime of 0.86 (the measured daytime $\Delta^{17}O(NO_2)$ mean value is (33.5 ± 3.9) ‰) meaning that 86 % of NO_2 is formed via R3 (oxidation of NO by O_3). The mean estimated RO_2 concentration is (14.8 ± 12.5) pmol mol^{-1}. Note that RO_2 = 0 pmol mol^{-1} for the 09:00-12:00 interval originates from our assumption of α = 1 for our highest $\Delta^{17}O(NO_2)$ value; in reality, it only means that RO_2 is so low that R3 ($NO + O_3$) ≫ R4 ($NO + RO_2$). Overall, our RO_2 values are found to be within the range of values measured at urban/peri-urban sites (see Table 2). However, RO_2 diurnal variation at our site do not follow the pattern of previous measurements which usually report a diurnal variation with a maximum varying from noon to early afternoon (Fuchs et al., 2008; Tan et al., 2017) whereas this study shows a maximal concentration in late afternoon. Further investigations with additional more accurate measurements and the use of a chemical box-model is needed to interpret this RO_2 behaviour.

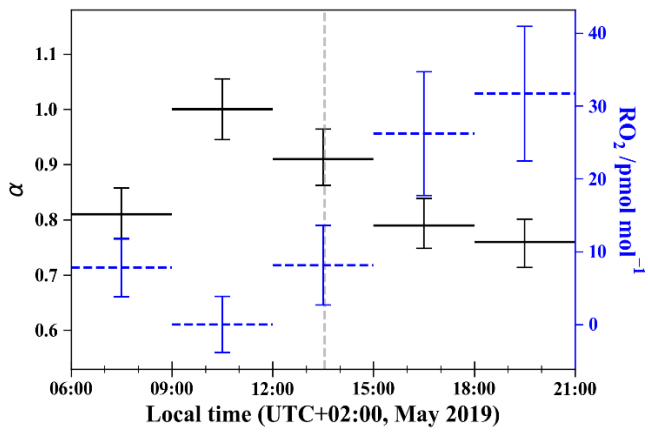

Figure 6: α (solid black slots) estimated from measured $\Delta^{17}O$ of atmospheric NO_2 in Grenoble and RO_2 concentrations (dashed blue slots) derived from Eq.(10). Error bars for α are derived from standard deviation of $\Delta^{17}O(NO_2)$ and $\Delta^{17}O(O_3^*)$ measured in Grenoble (Vicars and Savarino, 2014). RO_2 error bars are derived from O_3 measurement uncertainties and errors on α (by comparison, errors on reaction constants can be neglected). The dashed vertical line indicates the local solar noon.

https://doi.org/10.5194/acp-2020-1143
Preprint. Discussion started: 14 December 2020
© Author(s) 2020. CC BY 4.0 License.

Site	RO_2 /pmol mol^{-1}	Reference
Grenoble (2019, May)	0-35 (*)	This study
UK, suburban site (2003, July-August)	4-22	Emmerson et al. (2007)
Germany, suburban site (2005, July)	2-40	Fuchs et al. (2008)
Germany, rural site (1998, July-August)	2-50	Mihelcic et al. (2003)
USA, rural site (2002, May-June)	9-15	Ren et al. (2005)
China, rural site (2014, June-July)	7-37	Tan et al. (2017)

Table 2: Mean daytime RO_2 concentration ranges measured during field campaigns in various environments and seasons. (*) Derived from Eq.(6) using $\Delta^{17}O$ values of atmospheric NO_2 in Grenoble.

Morin et al. (2011) simulated the diurnal variation of $\Delta^{17}O(NO_2)$ in a remote marine boundary layer without the effect of emissions. They assumed $\Delta^{17}O(O_3)$ = 30 ‰ ($\Delta^{17}O_{NO+O3}(NO_2)$ = 45‰) resulting into higher overall $\Delta^{17}O(NO_2)$ values compared to our study. Their simulated $\Delta^{17}O(NO_2)$ exhibited large diurnal variations with maximum values at night (close to 41 ‰) and minimum values at noon of 28 ‰. This is consistent with RO_2 concentration reaching a maximum around local noon in clean environments. In contrast to their model simulations, our daytime $\Delta^{17}O(NO_2)$ measurements are higher than our nighttime measurements. We will show later that this difference originates from absence of NO emission in Morin et al., (2011) photochemical modelling.

4.2.3 $\Delta^{17}O_{night}(NO_2)$

Without photolysis at night and associated RO_2 production, ozone is the unique NO oxidant, and NO and NO_2 are no longer in photochemical equilibrium because NO_2 cannot be converted back into NO. As a result, the oxygen isotopic composition of NO_2 formed during the night is determined by the oxygen isotopic composition of emitted NO and O_3. Additionally, we need to determine the residual fraction $x(t)$ of NO_2 formed during the day that is still present at night in order to estimate the overall isotopic signature of NO_2 sampled at night following:

$$\Delta^{17}\mathrm{O}_{\mathrm{night}}(\mathrm{NO}_2) \approx x \times \Delta^{17}\mathrm{O}_{\mathrm{day}}(\mathrm{NO}_2) + \frac{(1-x)}{2} \times (\Delta^{17}\mathrm{O}_{\mathrm{NO+O_3}}(\mathrm{NO}_2) + \Delta^{17}\mathrm{O}(\mathrm{NO})) \quad (11)$$

with x being the residual fraction of NO_2 formed during the day to the total NO_2 measured at night and $(1-x)$ representing the fraction of the total NO_2 which has been produced during the night. NO is mainly emitted by combustion processes in which a nitrogen atom (from atmospheric N_2 or N present in fuel) is added to an oxygen atom formed by the thermal decomposition of O_2 (Zeldovich, 1946). With $\Delta^{17}O(O_2)$ being close to 0 ‰ (Barkan and Luz, 2003), NO is very likely to have a $\Delta^{17}O \approx 0$ ‰, or at least negligible compared to $\Delta^{17}O_{NO+O3}(NO_2)$. Using Eq.(11), along with a negligible isotope anomaly for NO, the evolution of $\Delta^{17}O(NO_2)$ over the night can be calculated. It is worth pointing out that the x fraction becomes very small at the end of the night allowing to simplify further Eq.(11) : $\Delta^{17}\mathrm{O}_{\mathrm{night}}(\mathrm{NO}_2) \approx \frac{1}{2} \times \Delta^{17}\mathrm{O}_{\mathrm{NO+O_3}}(\mathrm{NO}_2)$. Thus, if there are nighttime NO emissions, a measurement of $\Delta^{17}O(NO_2)$ at the end of the night is also an interesting way of deriving $\Delta^{17}O(O_3)$ which is difficult to measure directly. The nighttime variation of the x fraction is estimated considering that the nighttime

https://doi.org/10.5194/acp-2020-1143
Preprint. Discussion started: 14 December 2020
© Author(s) 2020. CC BY 4.0 License.

lifetime of NO_2 relative to oxidation via ozone and dry deposition is 7.2 hours (O_3 chemical sink is dominant over deposition by a factor > 10^4 with $k_{NO2+O3} = 1.4\times10^{-13}$ exp[−2470/T] cm^3 $molec^{-1}$ s^{-1} Atkinson et al., 2004; NO_2 dry velocity $V_d = 0.25$ cm s^{-1} Holland et al., 1999 and assuming a nighttime boundary layer height of 500 m). For the 00:00-05:00 interval, we calculate a mean value of $\Delta^{17}O(NO_2)$ = 19.9‰ (with an overall error of about 1.6 ‰) which is very close to our measured $\Delta^{17}O(NO_2)$ of 20.5 ‰. Overall, this first dataset of $\Delta^{17}O(NO_2)$ nighttime measurements comes to confirm our understanding of nighttime NO_2 formation (Alexander et al., 2020; Michalski et al., 2014). NO emissions in urban areas have a very significant influence on $\Delta^{17}O(NO_2)$ leading to a behaviour in opposition to the one observed in remote locations. As illustrated by Morin et al. (2011), $\Delta^{17}O(NO_2)$ is predicted to be maximal at night in remote areas where NO emissions are negligible, reflecting the isotopic signature of NO_2 at sunset. In areas where nighttime NO emissions are high, nighttime $\Delta^{17}O(NO_2)$ can be up to a factor of two smaller than in remote areas.

5 Conclusion

The primary goal of this preliminary work was to address an efficient and portable sampling system for atmospheric NO_2 fitting with accurate isotopic analysis of double nitrogen and triple oxygen isotopes. First simultaneous measurements of the multi-isotopic composition ($\delta^{15}N$, $\delta^{18}O$, and $\Delta^{17}O$) of atmospheric NO_2 are reported here, notably at relatively high temporal resolution (3 h). Over the course of more than one day in the Grenoble urban/suburban environment, $\delta^{15}N$ values of NO_2 shows little variation from −11.8 to −4.9 ‰ with negligible N isotope fractionations between NO and NO_2 due to high NO_2/NO_x ratios. NO_x emissions main sources are estimated using a stable isotope model indicating a high probability of the predominance of traffic NO_x emissions in this area. We found $\Delta^{17}O$ to vary diurnally with a maximum daytime value of (39.2 ± 1.7) ‰ and a minimum night-time value of (20.5 ± 1.7) ‰. At photo-stationary state, high $\Delta^{17}O(NO_2)$ values results from the ozone predominance in NO oxidation pathways whereas lower values reflect the influence of peroxy radicals. We estimate from $\Delta^{17}O(NO_2)$ measurements that 86 % of NO_2 produced by day originates from the oxidation of NO by O_3. Moreover, a mean daytime peroxy radical concentration of (14.8 ± 13.5) pmol mol^{-1} is derived from the oxygen isotopic measurements. At night, NO_x photochemistry shutdowns and hence $\Delta^{17}O(NO_2)$ decreases under the growing influence of the isotopic footprint from NO emitted by night. Our $\Delta^{17}O(NO_2)$ measured during the middle/end of the night is quantitatively consistent with typical values of $\Delta^{17}O(O_3)$. The overall agreement between our measured values and laboratory studies argue for high accuracy of our analytical field sampling method however nitrite standards with higher $\Delta^{17}O$ value must be developed to further improve data calibration. This work sheds light on the sensitivity of NO_2 isotopic signature to the atmospheric chemical regimes and emissions of the local environment. This isotopic approach can be applied to various environment in order to probe further the oxidative chemistry and help to constrain the NO_x fate in a more quantitative way.

In the future, this method should be extended with a modelling tool such as a photochemical box model including isotopic anomaly transfers and local emissions in order to solve persistent issues of atmospheric oxidation mechanisms. Moreover,

https://doi.org/10.5194/acp-2020-1143
Preprint. Discussion started: 14 December 2020
© Author(s) 2020. CC BY 4.0 License.

samplings and multi-isotopic analysis of atmospheric nitrate performed in parallel to those of NO_2 would certainly be of interest for the study of the full reactive nitrogen cycle.

Appendix A: Isotopic standards and calibration

This method of analysis induces isotope fractionations during NO_2^-/N_2O conversion and ionization in the spectrometer, as well as isotope exchanges between NO_2^- and its medium. Indeed, while isotope exchanges between nitrite and its matrix are minimized due to the basic pH, the chemistry required to convert nitrite to N_2O involves a step in an acidic medium that promotes an exchange of oxygen isotopes (Casciotti et al., 2007). In order to eliminate the effects of these isotope splits, the system is calibrated using standards of known isotopic composition, which are subjected to the same treatment as the samples. This is called the identical treatment principle (Brand, 1996). By subjecting compounds of known isotopic composition to the same treatment as the samples, the isotope fractionation induced by the manipulations can be estimated and the values of the samples can be corrected. Standards are first dissolved in a basic aqueous medium (pH = 12) and then, from this stock solution, five series of each standard are prepared in several concentration ranges, namely, 40 nmol, 80 nmol, 100 nmol, 120 nmol and 150 nmol in order to estimate the effects of the concentration of a material on its isotopic measurement. The matrix used for their preparation is the same as that of the samples, i.e. a mixture of KOH 2M/guaiacol in Milli-Q water. Correction factors are obtained by linear regression between the raw and the expected values of $\delta^{15}N$, $\delta^{18}O$ and $\delta^{17}O$ of the standards. Three international references of known $\delta^{15}N$ and $\delta^{18}O$ values are used for this work. These are nitrite salts, named RSIL-N7373, RSIL-N10219 and RSIL-N23 with respective $\delta^{15}N/\delta^{18}O$ values of –79.6/4.2 ‰, 2.8/88.5 ‰, and 3.7/11.4 ‰. Although the three standards cover a wide range of isotopic composition in $\delta^{15}N$ and $\delta^{18}O$, they do not have an isotopic anomaly in ^{17}O. As we are not aware of any available international reference nitrite standards with a known ^{17}O anomaly, we are currently in the process of manufacturing our own standards. As this step is still under development, and in order to be able to assess the accuracy of our ^{17}O measurements of atmospheric NO_2 samples, we have estimated the isotope fractionation that ^{17}O undergoes during the analysis. RSIL-N7373 and RSIL-N23 standards having a $\Delta^{17}O$ = 0 ‰ we estimate their ^{17}O composition such that $\delta^{17}O = 0.52 \times \delta^{18}O$. For standard RSIL-N10219, we measure a negative $\Delta^{17}O$ around −7 ‰. We therefore apply the mass independent relation such that $\delta^{17}O_{std}(\text{RSIL-N10219}) = \Delta^{17}O_{raw}(\text{RSIL-N10219}) + 0.5 \times \delta^{18}O_{std}(\text{RSIL-N10219})$.

The isotopic exchange of ^{18}O is estimated at 11 % for standards at 100 nmol (Fig. A1) which is in line with Kobayashi et al., 2020 who have estimated the degree of O isotope exchange in the azide method between H_2O and NO_2^- to (10.8 ± 0.3) %. The ^{15}N calibration curve allows us to ensure a good fractionation rate during the analysis. Indeed, given the 1:1 association of the nitrogen atoms of nitrite and azide, the theoretical value of the calibration slope must be 0.5. The slight deviation from our measured value can be attributed to a blank effect, estimated here at 2 % of the size of the standards (6 % for those at 40 nmol).

https://doi.org/10.5194/acp-2020-1143
Preprint. Discussion started: 14 December 2020
© Author(s) 2020. CC BY 4.0 License.

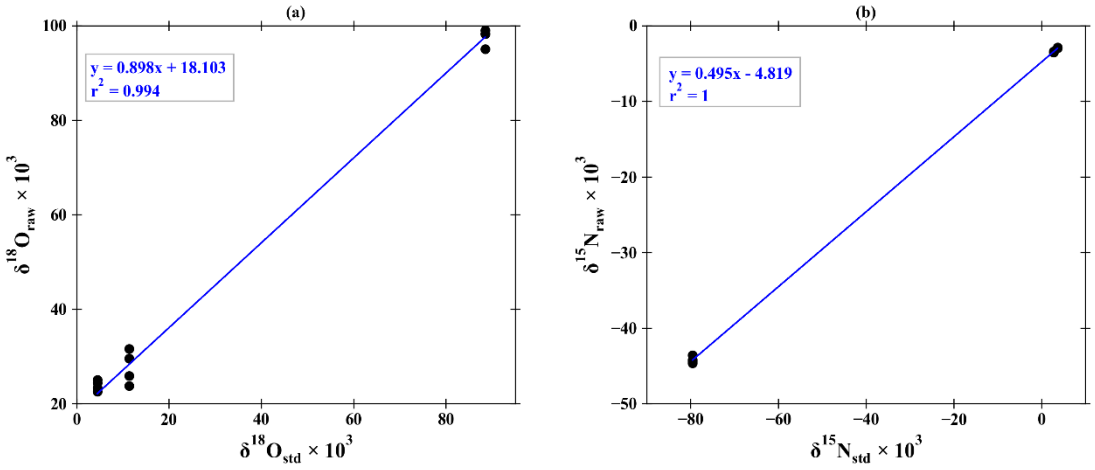

Figure A1: Calibration of (a) ^{18}O and (b) ^{15}N with nitrite standards at 100 nmol measured by the chemical azide method. The measured $\delta^{18}O$ ($\delta^{18}O_{raw}$) and $\delta^{15}N$ ($\delta^{15}N_{raw}$) values of NO_2^- standards are plotted against their certified reference $\delta^{18}O$ ($\delta^{18}O_{std}$) and $\delta^{15}N$ ($\delta^{15}N_{std}$) values.

Appendix B: Isotopic standards and calibration

Oxygen isotopes in nitrites are very labile (Böhlke et al., 2007) but the basic pH of the eluent limits isotopic exchanges. To ensure isotopic integrity from denuders extraction to analysis by IRMS, we followed Walters et al. (2018) procedure to quantify isotopic exchanges that might occur with the eluted matrix during storage. Thus, three solutions containing each 500 nmol of KNO_2 salts (RSIL-N7373, RSIL-N10219 and RSIL-N23) were prepared in the eluted matrix and kept frozen. 100 nmol were collected from time to time from the individual solutions, analysed and refrozen until the next analysis. We monitored the nitrite standards isotopic composition prepared in the eluted guaiacol matrix during 22 days. The temporal evolution of the $\delta^{17}O$, $\delta^{18}O$ and $\Delta^{17}O$ differences between our measurements of RSIL standards (prepared in the KOH/guaiacol eluted matrix) and their certified reference values is plotted in Figure B1. It represents the temporal drift of the isotopic signal with respect to reference values. If the deviation is constant, it means that the isotopic signal is not degraded with time and its standard deviation is considered as the uncertainty in our $\delta^{17}O(NO_2)$ and $\delta^{18}O(NO_2)$ measurements. As shown in Fig. B1, deviations of the three standards were stable over the 22-days experiment with an overall mean of (1.1 ± 0.8) ‰, (2.3 ± 1.8) ‰, and (–0.1 ± 0.3) ‰ for $\delta^{17}O$, $\delta^{18}O$ and $\Delta^{17}O$ respectively. Note that RSIL-N10219 shows higher $\delta^{17}O$ and $\delta^{18}O$ residuals than the two other standards. The reason for this difference of behaviour is still not fully understood. As residuals remain steady over several weeks, we consider this method suitable for the oxygen analysis of NO_2 and the uncertainties applied to our isotopic measurements are reported as the propagation error of the mean measurement uncertainty and the mean uncertainty resulting from NO_2^- storage. In our study, average uncertainties on $\delta^{17}O$, $\delta^{18}O$, and $\Delta^{17}O$ are estimated to be ± 1.1, ± 2.5 and ±1.7 ‰, respectively (1σ uncertainties).

https://doi.org/10.5194/acp-2020-1143
Preprint. Discussion started: 14 December 2020
© Author(s) 2020. CC BY 4.0 License.

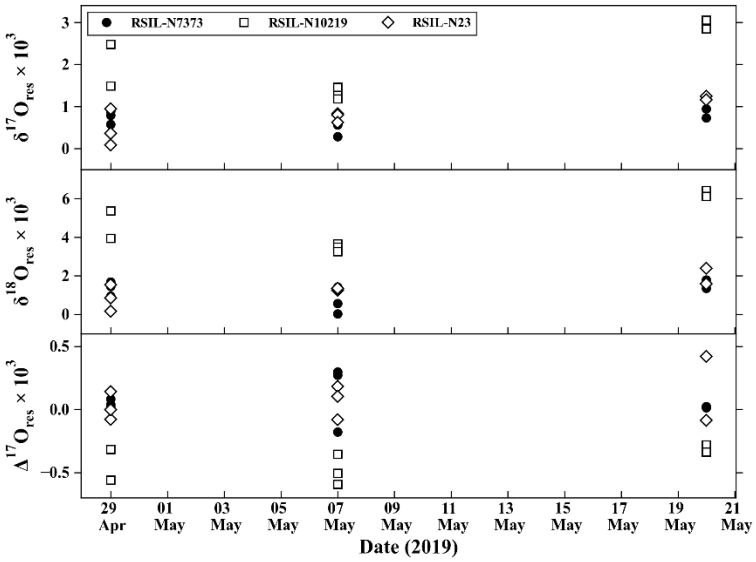

Figure B1: Temporal evolution of $\delta^{17}O$, $\delta^{18}O$ and $\Delta^{17}O$ differences between our measurements of RSIL standards (prepared in the KOH/guaiacol eluted matrix) and their certified reference values. Error bars derived from measurement uncertainties are approximately equivalent to the size of the markers.

Author contribution. Sampling and analysis protocol were developed by SA under the supervision of JS. NC and AB contributed with technical and knowledge support to SA for isotopic mass spectrometry and more general atmospheric measurements. SB and JS, supervisors of SA PhD Thesis, helped SA in interpreting the results and writing the manuscript.

Competing interests. The authors have no conflict of interests to report.

Acknowlegements. The authors acknowledge the support of the ALPACA program (Alaskan Layered Pollution and Arctic Chemical Analysis) funded by two French research organisms: the French polar institute (IPEV, Institut polaire français Paul-Emile Victor) and INSU-CNRS (National Institute of Sciences of the Universe) via its national LEFE program (Les Enveloppes Fluides et l'Environnement). This work benefited from the IGE infrastructures and laboratory platform PANDA which are partially supported by the ANR project ANR-15-IDEX-02 and Labex OSUG@2020, Investissements d'avenir – ANR10 LABX56. We would like to thank E. Gauthier, S. Darfeuil and P. Akers for help with laboratory work and more general scientific advises.

https://doi.org/10.5194/acp-2020-1143
Preprint. Discussion started: 14 December 2020
© Author(s) 2020. CC BY 4.0 License.

References

Alexander, B., Hastings, M. G., Allman, D. J., Dachs, J., Thornton, J. A. and Kunasek, S. A.: Quantifying atmospheric nitrate formation pathways based on a global model of the oxygen isotopic composition (Δ^{17}O) of atmospheric nitrate, Atmospheric Chemistry and Physics, 9(14), 5043–5056, doi:https://doi.org/10.5194/acp-9-5043-2009, 2009.

Alexander, B., Sherwen, T., Holmes, C. D., Fisher, J. A., Chen, Q., Evans, M. J. and Kasibhatla, P.: Global inorganic nitrate production mechanisms: comparison of a global model with nitrate isotope observations, Atmospheric Chemistry and Physics, 20(6), 3859–3877, doi:https://doi.org/10.5194/acp-20-3859-2020, 2020.

Assonov, S. S. and Brenninkmeijer, C. a. M.: Reporting small Δ17O values: existing definitions and concepts, Rapid Communications in Mass Spectrometry, 19(5), 627–636, doi:https://doi.org/10.1002/rcm.1833, 2005.

Atkinson, R., Baulch, D. L., Cox, R. A., Hampson, R. F., Kerr, J. A., Rossi, M. J. and Troe, J.: Evaluated Kinetic, Photochemical and Heterogeneous Data for Atmospheric Chemistry: Supplement V. IUPAC Subcommittee on Gas Kinetic Data Evaluation for Atmospheric Chemistry, Journal of Physical and Chemical Reference Data, 26(3), 521–1011, doi:10.1063/1.556011, 1997.

Atkinson, R., Baulch, D. L., Cox, R. A., Crowley, J. N., Hampson, R. F., Hynes, R. G., Jenkin, M. E., Rossi, M. J. and Troe, J.: Evaluated kinetic and photochemical data for atmospheric chemistry: Volume I - gas phase reactions of O_x, HO_x, NO_x and SO_x species, Atmospheric Chemistry and Physics, 4(6), 1461–1738, doi:https://doi.org/10.5194/acp-4-1461-2004, 2004.

Barkan, E. and Luz, B.: High-precision measurements of $^{17}O/^{16}O$ and $^{18}O/^{16}O$ of O_2 and O_2/Ar ratio in air, Rapid Commun. Mass Spectrom., 17(24), 2809–2814, doi:10.1002/rcm.1267, 2003.

Barré, J., Petetin, H., Colette, A., Guevara, M., Peuch, V.-H., Rouil, L., Engelen, R., Inness, A., Flemming, J., Pérez García-Pando, C., Bowdalo, D., Meleux, F., Geels, C., Christensen, J. H., Gauss, M., Benedictow, A., Tsyro, S., Friese, E., Struzewska, J., Kaminski, J. W., Douros, J., Timmermans, R., Robertson, L., Adani, M., Jorba, O., Joly, M. and Kouznetsov, R.: Estimating lockdown induced European NO_2 changes, Atmospheric Chemistry and Physics Discussions, 1–28, doi:https://doi.org/10.5194/acp-2020-995, 2020.

Böhlke, J. K., Smith, R. L. and Hannon, J. E.: Isotopic Analysis of N and O in Nitrite and Nitrate by Sequential Selective Bacterial Reduction to N_2O, Analytical Chemistry, 79(15), 5888–5895, doi:10.1021/ac070176k, 2007.

Brand, W. A.: High Precision Isotope Ratio Monitoring Techniques in Mass Spectrometry, Journal of Mass Spectrometry, 31(3), 225–235, doi:10.1002/(SICI)1096-9888(199603)31:3<225::AID-JMS319>3.0.CO;2-L, 1996.

Brown, S. S.: Variability in Nocturnal Nitrogen Oxide Processing and Its Role in Regional Air Quality, Science, 311(5757), 67–70, doi:10.1126/science.1120120, 2006.

Buttini, P., Di Palo, V. and Possanzini, M.: Coupling of denuder and ion chromatographic techniques for NO_2 trace level determination in air, Science of The Total Environment, 61, 59–72, doi:10.1016/0048-9697(87)90356-1, 1987.

Casciotti, K. L., Sigman, D. M., Hastings, M. G., Böhlke, J. K. and Hilkert, A.: Measurement of the oxygen isotopic composition of nitrate in seawater and freshwater using the denitrifier method, Analytical Chemistry, 74(19), 4905–4912, doi:10.1021/ac020113w, 2002.

Crutzen, P. J.: My life with O_3, NO_x and other YZO_x compounds (Nobel lecture), Angewandte Chemie Int. Ed. Engl., 35, 1759 – 1776, 1996.

Dahal, B. and Hastings, M. G.: Technical considerations for the use of passive samplers to quantify the isotopic composition of NO_x and NO_2 using the denitrifier method, Atmospheric Environment, 143, 60–66, doi:10.1016/j.atmosenv.2016.08.006, 2016.

Davidson, E. A. and Kingerlee, W.: A global inventory of nitric oxide emissions from soils, Nutrient Cycling in Agroecosystems, 48(1), 37–50, doi:10.1023/A:1009738715891, 1997.

Dennison, P., Charoensiri, K., Roberts, D., Peterson, S. and Green, R.: Wildfire temperature and land cover modeling using hyperspectral data, Remote Sensing of Environment, 100(2), 212–222, doi:10.1016/j.rse.2005.10.007, 2006.

EPA IsoSource Model: Stable Isotope Mixing Models for Estimating Source Proportions, [online] Available from: https://www.epa.gov/eco-research/stable-isotope-mixing-models-estimating-source-proportions (Accessed 15 October 2020), 2003.

Finlayson-Pitts, B. J. and Pitts, J. N.: Chemistry of the Upper and Lower Atmosphere, Elsevier., 2000.

Freyer, H. D., Kley, D., Volz-Thomas, A. and Kobel, K.: On the interaction of isotopic exchange processes with photochemical reactions in atmospheric oxides of nitrogen, Journal of Geophysical Research: Atmospheres, 98(D8), 14791–14796, doi:10.1029/93JD00874, 1993.

Fuchs, H., Holland, F. and Hofzumahaus, A.: Measurement of tropospheric RO_2 and HO_2 radicals by a laser-induced fluorescence instrument, Review of Scientific Instruments, 79(8), 084104, doi:10.1063/1.2968712, 2008.

Galloway, J. N., Dentener, F. J., Capone, D. G., Boyer, E. W., Howarth, R. W., Seitzinger, S. P., Asner, G. P., Cleveland, C. C., Green, P. A., Holland, E. A., Karl, D. M., Michaels, A. F., Porter, J. H., Townsend, A. R. and Vöosmarty, C. J.: Nitrogen Cycles: Past, Present, and Future, Biogeochemistry, 70(2), 153–226, doi:10.1007/s10533-004-0370-0, 2004.

Geng, F., Tie, X., Xu, J., Zhou, G., Peng, L., Gao, W., Tang, X. and Zhao, C.: Characterizations of ozone, NO_x and VOCs measured in Shanghai, China, Atmospheric Environment, 42(29), 6873–6883, doi:10.1016/j.atmosenv.2008.05.045, 2008.

Harris, G. W., Carter, W. P. L., Winer, A. M., Pitts, J. N., Platt, Ulrich. and Perner, Dieter.: Observations of nitrous acid in the Los Angeles atmosphere and implications for predictions of ozone-precursor relationships, Environ. Sci. Technol., 16(7), 414–419, doi:10.1021/es00101a009, 1982.

Holland, E. A., Dentener, F. J., Braswell, B. H. and Sulzman, J. M.: Contemporary and pre-industrial global reactive nitrogen budgets, Biogeochemistry, 46(1), 7–43, doi:10.1023/A:1006148011944, 1999.

Jacob, D. J.: Introduction to Atmospheric Chemistry, Princeton University Press [online] Available from: http://acmg.seas.harvard.edu/publications/jacobbook/bookchap11.pdf (Accessed 17 February 2020), 1999.

Jin, S. and Demerjian, K.: A photochemical box model for urban air quality study, Atmospheric Environment. Part B. Urban Atmosphere, 27(4), 371–387, doi:10.1016/0957-1272(93)90015-X, 1993.

Johnston, J. C. and Thiemens, M. H.: The isotopic composition of tropospheric ozone in three environments, J. Geophys. Res., 102(D21), 25395–25404, 1997.

Kaiser, J., Röckmann, T. and Brenninkmeijer, C. A. M.: Contribution of mass-dependent fractionation to the oxygen isotope anomaly of atmospheric nitrous oxide, Journal of Geophysical Research: Atmospheres, 109(D3), D03305, doi:10.1029/2003JD004088, 2004.

Kaiser, J., Hastings, M. G., Houlton, B. Z., Röckmann, T. and Sigman, D. M.: Triple oxygen isotope analysis of nitrate using the denitrifier method and thermal decomposition of N_2O, Anal. Chem., 79(2), 599–607, doi:10.1021/ac061022s, 2007.

Kaye, J. A.: Mechanisms and observations for isotope fractionation of molecular species in planetary atmospheres, Reviews of Geophysics, 25(8), 1609–1658, doi:10.1029/RG025i008p01609, 1987.

Klein, A., Ravetta, F., Thomas, J. L., Ancellet, G., Augustin, P., Wilson, R., Dieudonné, E., Fourmentin, M., Delbarre, H. and Pelon, J.: Influence of vertical mixing and nighttime transport on surface ozone variability in the morning in Paris and the surrounding region, Atmospheric Environment, 197, 92–102, doi:10.1016/j.atmosenv.2018.10.009, 2019.

Kleinman, L. I., Daum, P. H., Lee, Y.-N., Nunnermacker, L. J., Springston, S. R., Weinstein-Lloyd, J. and Rudolph, J.: Ozone production efficiency in an urban area, Journal of Geophysical Research: Atmospheres, 107(D23), 4733, doi:10.1029/2002JD002529, 2002.

Kobayashi, K., Fukushima, K., Onishi, Y., Nishina, K., Makabe, A., Yano, M., Wankel, S. D., Koba, K. and Okabe, S.: Influence of δ18O of water on measurements of δ18O of nitrite and nitrate, Rapid Communications in Mass Spectrometry, n/a(n/a), doi:10.1002/rcm.8979, 2020.

Krankowsky, D., Bartecki, F., Klees, G. G., Mauersberger, K., Schellenbach, K. and Stehr, J.: Measurement of heavy isotope enrichment in tropospheric ozone, Geophys. Res. Lett., 22(13), 1713–1716, 1995.

Largeron, Y. and Staquet, C.: Persistent inversion dynamics and wintertime PM10 air pollution in Alpine valleys, Atmospheric Environment, 135, 92–108, doi:10.1016/j.atmosenv.2016.03.045, 2016.

Leighton, P. A.: Photochemistry of Air Pollution., Academic Press, 66(3), 279–279, doi:10.1002/bbpc.19620660323, 1961.

Li, J., Zhang, X., Orlando, J., Tyndall, G. and Michalski, G.: Quantifying the nitrogen isotope effects during photochemical equilibrium between NO and NO_2: implications for $\delta^{15}N$ in tropospheric reactive nitrogen, Atmospheric Chemistry and Physics, 20(16), 9805–9819, doi:https://doi.org/10.5194/acp-20-9805-2020, 2020.

Li, W., Ni, B. L., Jin, D. Q. and Zhang, Q. G.: Measurement of the absolute abundance of Oxygen-17 in SMOW, Kexue Tongboa, Chinese Science Bulletin, 33 (19), 1610–1613, doi:10.1360/sb1988-33-19-1610, 1988.

Liao, H. and Seinfeld, J. H.: Global impacts of gas-phase chemistry-aerosol interactions on direct radiative forcing by anthropogenic aerosols and ozone, Journal of Geophysical Research: Atmospheres, 110(D18), doi:10.1029/2005JD005907, 2005.

Lyons, J. R.: Transfer of mass-independent fractionation in ozone to other oxygen-containing radicals in the atmosphere, Geophysical Research Letters, 28(17), 3231–3234, doi:10.1029/2000GL012791, 2001.

Mariotti, A.: Natural 15 N abundance measurements and atmospheric nitrogen standard calibration, Nature, 311(5983), 251, doi:10.1038/311251a0, 1984.

Mayer, H.: Air pollution in cities, Atmospheric Environment, 33(24), 4029–4037, doi:10.1016/S1352-2310(99)00144-2, 1999.

McIlvin, M. R. and Altabet, M. A.: Chemical Conversion of Nitrate and Nitrite to Nitrous Oxide for Nitrogen and Oxygen Isotopic Analysis in Freshwater and Seawater, Analytical Chemistry, 77(17), 5589–5595, doi:10.1021/ac050528s, 2005.

Michalski, G., Scott, Z., Kabiling, M. and Thiemens, M. H.: First measurements and modeling of $\Delta^{17}O$ in atmospheric nitrate., Geophysical Research Letters, 30(16), doi:10.1029/2003GL017015, 2003.

Michalski, G., Bhattacharya, S. K. and Girsch, G.: NO_x cycle and the tropospheric ozone isotope anomaly: an experimental investigation, Atmospheric Chemistry and Physics, 14(10), 4935–4953, doi:10.5194/acp-14-4935-2014, 2014.

Miller, D. J., Wojtal, P. K., Clark, S. C. and Hastings, M. G.: Vehicle NOx emission plume isotopic signatures: Spatial variability across the eastern United States, Journal of Geophysical Research: Atmospheres, 122(8), 4698–4717, doi:10.1002/2016JD025877, 2017.

Monks, P. S.: Gas-phase radical chemistry in the troposphere, Chem. Soc. Rev., 34(5), 376–395, doi:10.1039/B307982C, 2005.

Morin, S.: Analyse de la composition isotopique de l'ion nitrate dans la basse atmosphère polaire et marine. Science de la Terre, PhD-Thesis, Université Paris-Est, France., 2008.

Morin, S., Savarino, J., Bekki, S., Gong, S. and Bottenheim, J. W.: Signature of Arctic surface ozone depletion events in the isotope anomaly ($\Delta^{17}O$) of atmospheric nitrate, Atmos. Chem. Phys., 7, 1451–1469, doi:10.5194/acp-7-1451-2007, 2007.

Morin, S., Sander, R. and Savarino, J.: Simulation of the diurnal variations of the oxygen isotope anomaly ($\Delta^{17}O$) of reactive atmospheric species, Atmospheric Chemistry and Physics, 11(8), 3653–3671, doi:https://doi.org/10.5194/acp-11-3653-2011, 2011.

Nash, T.: An efficient absorbing reagent for nitrogen dioxide, Atmospheric Environment (1967), 4(6), 661–665, doi:10.1016/0004-6981(70)90039-9, 1970.

Phillips, D. L. and Gregg, J. W.: Source partitioning using stable isotopes: coping with too many sources, Oecologia, 136(2), 261–269, doi:10.1007/s00442-003-1218-3, 2003.

Prinn, R. G.: The Cleasing Capacity of the Atmosphere, Annual Review of Environment and Resources, 28(1), 29–57, doi:10.1146/annurev.energy.28.011503.163425, 2003.

Röckmann, T., Kaiser, J., Crowley, J. N., Brenninkmeijer, C. A. M. and Crutzen, P. J.: The origin of the anomalous or "mass-independent" oxygen isotope fractionation in tropospheric N_2O, Geophysical Research Letters, 28(3), 503–506, doi:10.1029/2000GL012295, 2001.

Røyset, O.: Comparison of passive and active sampling methods for the determination of nitrogen dioxide in urban air, Fresenius' Journal of Analytical Chemistry, 360(1), 69–73, doi:10.1007/s002160050644, 1998.

Savarino, J., Bhattacharya, S. K., Morin, S., Baroni, M. and Doussin, J.-F.: The $NO+O_3$ reaction: A triple oxygen isotope perspective on the reaction dynamics and atmospheric implications for the transfer of the ozone isotope anomaly, J. Chem. Phys., 128(19), 194303, doi:10.1063/1.2917581, 2008.

Seinfeld, J. H. and Pandis, S. N.: Atmospheric chemistry and physics: from air pollution to climate change, 2nd ed., Wiley, Hoboken, NJ., 2006.

Tan, Z., Fuchs, H., Lu, K., Hofzumahaus, A., Bohn, B., Broch, S., Dong, H., Gomm, S., Häseler, R., He, L., Holland, F., Li, X., Liu, Y., Lu, S., Rohrer, F., Shao, M., Wang, B., Wang, M., Wu, Y., Zeng, L., Zhang, Y., Wahner, A. and Zhang, Y.: Radical chemistry at a rural site (Wangdu) in the North China Plain: observation and model calculations of OH, HO_2 and RO_2 radicals, Atmospheric Chemistry and Physics, 17(1), 663–690, doi:https://doi.org/10.5194/acp-17-663-2017, 2017.

Thiemens, M. H.: Mass-Independent Isotope Effects in Planetary Atmospheres and the Early Solar System, Science, 283, 341–345, doi:10.1126/science.283.5400.341, 1999.

Thiemens, M. H.: History and Applications of Mass-independent Isotope Effects, Annual Review of Earth and Planetary Sciences, 34(1), 217–262, doi:10.1146/annurev.earth.34.031405.125026, 2006.

Thiemens, M. H. and Heidenreich, J. E.: The Mass-Independent Fractionation of Oxygen: A Novel Isotope Effect and Its Possible Cosmochemical Implications, Science, 219, 1073–1075, doi:10.1126/science.219.4588.1073, 1983.

Tie, X., Madronich, S., Li, G., Ying, Z., Zhang, R., Garcia, A. R., Lee-Taylor, J. and Liu, Y.: Characterizations of chemical oxidants in Mexico City: A regional chemical dynamical model (WRF-Chem) study, Atmospheric Environment, 41(9), 1989–2008, doi:10.1016/j.atmosenv.2006.10.053, 2007.

Urey, H. C.: The thermodynamic properties of isotopic substances, J. Chem. Soc., (0), 562–581, doi:10.1039/JR9470000562, 1947.

Velasco, E., Márquez, C., Bueno, E., Bernabé, R. M., Sánchez, A., Fentanes, O., Wöhrnschimmel, H., Cárdenas, B., Kamilla, A., Wakamatsu, S. and Molina, L. T.: Vertical distribution of ozone and VOCs in the low boundary layer of Mexico City, Atmospheric Chemistry and Physics, 8(12), 3061–3079, doi:https://doi.org/10.5194/acp-8-3061-2008, 2008.

Vicars, W. C. and Savarino, J.: Quantitative constraints on the ^{17}O-excess (Δ^{17}O) signature of surface ozone: Ambient measurements from 50°N to 50°S using the nitrite-coated filter technique, Geochimica et Cosmochimica Acta, 135, 270–287, doi:10.1016/j.gca.2014.03.023, 2014.

Villena, G., Kleffmann, J., Kurtenbach, R., Wiesen, P., Lissi, E., Rubio, M. A., Croxatto, G. and Rappenglück, B.: Vertical gradients of HONO, NO_x and O_3 in Santiago de Chile, Atmospheric Environment, 45(23), 3867–3873, doi:10.1016/j.atmosenv.2011.01.073, 2011.

Walters, W. W., Tharp, B. D., Fang, H., Kozak, B. J. and Michalski, G.: Nitrogen isotope composition of thermally produced NO_x from various fossil-fuel combustion sources, Environmental Science & Technology, 49(19), 11363–11371, doi:10.1021/acs.est.5b02769, 2015.

Walters, W. W., Fang, H. and Michalski, G.: Summertime diurnal variations in the isotopic composition of atmospheric nitrogen dioxide at a small midwestern United States city, Atmospheric Environment, 179, 1–11, doi:10.1016/j.atmosenv.2018.01.047, 2018.

Williams, E. L. and Grosjean, D.: Removal of atmospheric oxidants with annular denuders, Environmental Science & Technology, 24(6), 811–814, doi:10.1021/es00076a002, 1990.

Young, G. L.: NO_x formation in rotary kilns producing cement clinker applicable NO_x control techniques and cost effectiveness of these control techniques, in: Conference record- IEEE Cement Industry Technical Conference, IEEE, Piscataway NJ, U., 239–254, doi:10.1109/CITCON.2002.1006510, 2002.

Zeldovich, Y. B.: The Oxidation of Nitrogen in Combustion and Explosions, Acta Physicochimica, Academy of Sciences U.S.S.R., 21, 577–628, 1946.